Broadband Dielectric Spectroscopy On the Molecular Dynamics in Different Generations of Hyperbranched Polyester

Gamal Turky,[1] Shereen S. Shaaban,[1] Andreas Schöenhals[2]

[1]Microwave Physics and Dielectrics, National Research Center, Dokki, Cairo, Egypt
[2]Federal Institute of Materials Research and Testing FG:VI.3, D-12205, Berlin, Germany

ABSTRACT: Dielectric spectroscopy (10^{-2} Hz to 10^6 Hz) was employed to investigate the molecular dynamics of hyperbranched polyesters where the number of the generation is systematically varied from 2 to 5. As a first result, the dielectric properties depends strongly on the generation of the hyperbranched polymers. For higher generations (3 to 5) at temperatures below T_g two relaxation processes are observed, a γ-process at lower temperatures and a β-process at higher ones. The apparent activation energies are around 100 kJ/mol which seems to be too high for truly localized processes. For the Generation 2, only the γ-process is observed. For all investigated polymers the dielectric α-relaxation could not be observed because of strong conductivity effects. Therefore, the conductivity is systematically analyzed which obeys the peculiarities found to be characteristic for semiconducting disordered materials. Especially, the Barton/Nakajima/Namikawa relationship is found to be valid. © 2009 Wiley Periodicals, Inc. J Appl Polym Sci 113: 2477–2484, 2009

Key words: molecular dynamics; polyesters; relaxation; synthesis

INTRODUCTION

Dendrimers are highly branched, globular macromolecules with a great number of arms emanating from central core.[1,2] The stepwise synthesis of dendrimers affords molecules with highly regular branching pattern, a definite molecular weight, a low polydispersity index and a well-defined number of peripheral groups.[3]

In recent years, dendritics (dendrimers, hyper branched and star polymers) have shown promise for different applications for instance in fields ranging from gene delivery to magnetic resonance imaging to the development of vaccines, antiviral, antibacterial and anticancer therapeutics.[4–7]

A comparison of the features of dendritics with those of linear polymers shows that the dendritic architecture can provide several advantages for instance for drug delivery application. For example, the multivalency of dendritics can be used to attach several drug molecules, targeting groups and solubilizing groups to the periphery of the dendritics in a well defined manner. Furthermore, the more globular shape of dendritics, as opposed to the random coil structure of most linear polymers, could affect their biological properties, leading to the discovery of interesting effects related to macromolecular architecture.

Hyperbranched (hb) polymers on the other hand, can be synthesized by a one step method without many and tedious purifying techniques. This makes them advantageous over dendrimers in that sense. They retain the main features of dendritic macromolecules and show properties intermediate to those of dendritics and linear polymers.[8,9] These dominate the high potential for applications in, for example, coating and resin applications and as additives for linear polymers. Moreover, their use in high-tech applications, such as catalysis, microelectronics, thin-film technology, and sensorics as well as many other applications are increasing strongly.[10–29]

The field of aliphatic hb polyesters with hydroxyl groups at the peripheral surfaces is dominated by products based on bishydroxy- methyl propionic or dimethylol propionic acid (DMPA). With the commercially available Boltorn* brands (from Perstorp) prepared by $AB_2 + B_3$ approach with stepwise slow monomer addition as shown in Figure 1. They are polydisperse polymers i.e. no protection groups are used to control dendritic growth. Hyperbranched growth is instead controlled by stoichiometric ratios

Correspondence to: G. Turky (gamalturky@yahoo.com).
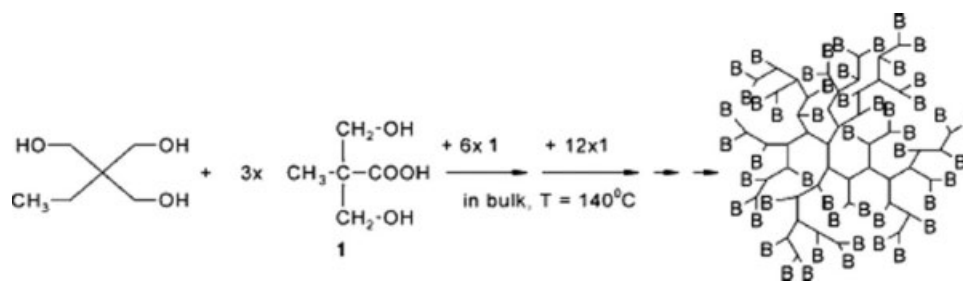
*Boltron is a trademark of Perstop.

Figure 1 Synthetic scheme for the synthesis of Boltron- type aliphatic polyesters with a core molecule (stepwise slow monomer addition). The B in the right formula symbolize the OH group.

of core-to-chain extenders and carefully chosen processing conditions to avoid side reactions. Perstorp hyperbranched polyesters resemble dendrimers in that sense that they consist of a core, from which branches extend, giving core/shell structure with a functional surface.

Dielectric Relaxation Spectroscopy (DRS) is a useful method to investigate structure property relationships of polymers.[30–43] This method is sensitive to molecular fluctuations of dipoles within the system. For polymers these fluctuations are related to the molecular mobility of groups (subglass processes), segments (segmental dynamics) or the whole polymer chain as well which are show up as different relaxation processes. For details see.[44,45] The fluctuations of dipoles are taken as a probe for structure.

Malmström et al.[46] found two relaxation processes below the glass transition temperature (subglass processes), for the fifth generation (H50) of hyperbranched polyester with hydroxyl units as the terminal groups: (a) a low temperature γ-process because of the fluctuations of hydroxyl groups, and (b) a β-process originating from the reorientation of the ester groups at higher temperatures than the former one. They do not report an α-relaxation process related to glassy (segmental) dynamics although the glass transition can be measured by thermal methods. The hiding of the α-relaxation is because of conductivity and/or electrode polarization effects which overlays this relaxation process. This seems to be a general feature for these aliphatic hb polyesters because this effect on the dynamic glass transition was also found for polyurethanes based on the 4th generation of hb polyester (trade name Boltorn® H40).[47] On the other hand, the glassy dynamics was investigated in the case of the linear/hb polyurethanes blends and in the polyurethanes networks[48–50] using dielectric spectroscopy.

Recently, thin films of *aromatic* hyper branched polyesters was investigated by Serghei et al.[51,52] using DRS to study confinement effects. Three relaxation processes namely; α, β, and γ were detected. A pronounced confinement effect on the alpha process was observed. With decreasing film thickness the slower

relaxation modes of the dynamic glass transition were gradually suppressed, resulting in an increase of the average relaxation rate and a decrease of the dielectric strength. On the other hand, an inverse trend was detected for the dilatometric glass transition. The divergence between the microscopic dynamics and macroscopic thermal expansion proves that different experimental techniques do not necessarily deliver similar results when applied in confinement.

The aim of the present study is to study the dynamics of a series of aliphatic hyper branched polyesters with hydroxyl group as terminal groups in dependence on the generation number (2nd to 5th), nomenclature as H20 to H50 in the text, in the bulk. The effect of molecular weight (generation number) on the molecular dynamics and the conductivity will be considered.

EXPERIMENTAL

Materials

The hyper branched polymers used in this study are aliphatic polyesters synthesized using ethoxylated pentaethritol as central cores and 2, 2–bis (methylol) propionic acid as dendritic units. They are polydisperse polymers, i.e. no protection groups are used to control dendritic grows. Hyperbranched growth is instead controlled by stoichiometric ratios of core-to-chain extenders and carefully chosen processing conditions to avoid side reactions. The materials are supplied by Perstorp, Sweden, under the trade name Boltorn H20 – H50 (indicating the second to the fifth generations). The glass transition temperatures for the investigated samples were found[8] by DSC to be 303, 308, 321, and 320 K with increasing number of generation. Size exclusion chromatography was applied to determine the molecular weights of these hyper branched polymers.[8] The molecular weights were found to be[8]: 2100, 3500, 5100, and 7500 g/mol, respectively. The products are all hydroxyl functional. Hydroxyl number, molecular weight and polydispersity of Boltorn polymers from the data sheet provided by Perstorp are presented in Ref. 53.

Dielectric measurements

The samples were pressed at a temperature of 333 K between two gold-plated stainless steel electrodes of 20 mm in diameter. Fused silica fibers with a diameter of 50 μm were used as spacer material (parallel plate capacitor geometry). The samples were annealed at temperatures above the glass transition temperature in vacuum for 12 h to remove water as much as possible.

The complex dielectric function

$$\varepsilon^*(\nu) = \varepsilon'(\nu) - i\varepsilon''(\nu), \tag{1}$$

where, ν is the frequency, ε' the real part, ε'' the imaginary or loss part, was measured in a frequency range from 10^9 to 10^6 Hz using a frequency response analyzer Solatron/Schlumberger FRA 1260 connected to a buffer amplifier of variable gain (Chelsea dielectric interface). The temperature of the samples was controlled by a custom-made gas jet heating system operated with liquid nitrogen. Before each frequency sweep the sample was thermally equilibrated at the selected temperature with a stability of 0.05 K. The temperature range of the measurements was limited up to 323 K or 333 K because of the melting of the samples.

RESULTS AND DISCUSSION

Figure 2 illustrates the dependence of imaginary part of the complex dielectric permittivity ε'' on temperature for the investigated samples for four different frequencies (log (ν[Hz]) = −0.5, 0.5, 3, and 5). The dielectric behavior for the lowest generation of the hb polymers (H20) is quite different from that of the higher ones. For the latter cases, at the lower frequency two relaxation processes are identified as peaks in ε''. The process at lower temperature (at about 220 K) is attributed according to the literature[8,54] to the motion of hydroxyl groups and is further called γ-process. The peak broadens and shifts to higher temperatures with increasing frequency as expected. The peak at higher temperature is sharper and has a higher intensity in comparison with the γ-process. Its maximum position is at about 280 and 300 K for the lower frequencies (log(ν [Hz]) = −0.5 and 0.5) and shifts outside of temperature window for the higher frequencies. Its maximum position is about 50 to 60 K lower than the glass transition temperature measured by DSC. This means that it could not be related to glassy dynamics (α-process). Therefore this process is assigned as β-process, which might originate from the orientation fluctuations of the ester groups. The β-process is overlaid by a conductivity contribution and/or electrode polarization effects which probably hides the expected peak because of the α-process related to the glass transi-

tion. For the sample H20 for the lower frequencies an abrupt increase of ε'' just above the temperatures of γ relaxation is observed. At moderate and higher frequencies (log (ν [Hz]) = 3 and 5) only the γ relaxation could be seen clearly here followed by a wing of the β relaxation peak and conductivity or/and electrode contributions.

Figure 3 gives the dielectric loss ε'' as a function of frequency at different temperatures ranging from 252 to 313 K. All investigated samples show the broad peak of the γ-process at temperatures below 273 K. No conductivity contribution could be considered here but only a wing of the β relaxation peak is observed within this temperature range. This relaxation peak shifts towards higher frequencies with increasing temperatures. The general inspection of Figures 2 and 3 shows that the values of ε'' at low frequencies and higher temperatures for the sample H30 are much lower than that of the other samples. This is most pronounced for the sample H20 showing a strong increase of the dielectric loss at low frequencies. That strong increase of ε'' with decreasing frequency is probably because of conductivity and/or electrode polarization for these polymers of special architecture. A clear relaxation peak (β-relaxation) at temperatures beginning from 273 K is observed which overlaid by dc conductivity for H40 and H50 samples. On the other hand, the loss peak of H20 is masked by the dc conductivity. No remarkable contribution of conductivity of sample H30 could be seen in both figures.

In the first part, the γ-Relaxation is discussed in detail for all samples where in the second part the β-process and the conductivity is analyzed.

γ-Relaxation

The model function of Havriliak–Negami (HN-function)[55] is fitted to the isothermal data[56] to describe the different relaxation processes and to extract the relaxation rate at maximum loss ν_p and the dielectric strength $\Delta\varepsilon$. The HN-function reads

$$\varepsilon^*_{\mathrm{HN}}(\nu) = \varepsilon_\infty + \frac{\Delta\varepsilon}{(1 + (i\frac{\nu}{\nu_0})^{\beta_{\mathrm{HN}}})^{\gamma_{\mathrm{HN}}}} \tag{2}$$

with the parameters $\Delta\varepsilon$-dielectric strength or intensity, ν_0 characteristic frequency which is related to the peak frequency ν_p but depends on the asymmetry parameter γ_{HN}[44] and $\varepsilon_\infty = \varepsilon'(\nu)$ for $\nu \gg \nu_p$. The fractional shape parameters β_{HN} and γ_{HN} describe the symmetric and asymmetric broadening of the complex dielectric function when compared with Debye formula. Because they are related to the slopes of log ε'' versus log ν for low and high frequencies with respect to ν_p $0 < \beta_{\mathrm{HN}} \leq 1$ and $0 < \beta_{\mathrm{HN}}$ $\gamma_{\mathrm{HN}} \leq 1$ holds.[44]

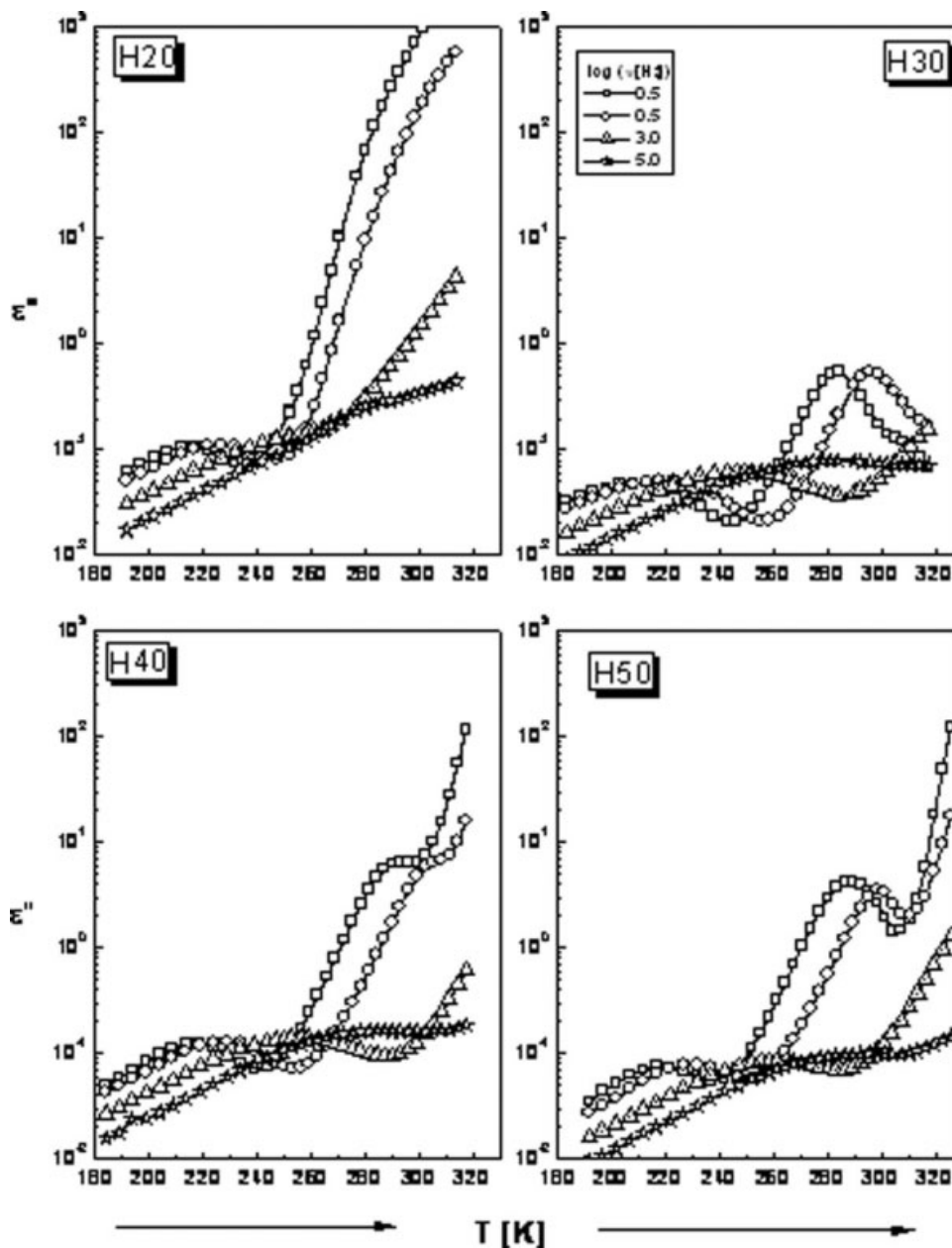**Figure 2**　ε'' versus temperature for the three label frequencies for the nvestigated samples.

The activation plot [Fig. 4] shows the temperature dependence of the relaxation rate, $\log \nu_p$, for γ-process of the four samples under consideration. The temperature dependence of $\log \nu_p$ for the gamma relaxation can be described by an Arrhenius relation.

$$\log(\upsilon_p) = \log \upsilon_\infty = \frac{\ln 10 E_A}{k_B T}, \qquad (3)$$

where, υ_∞ is the so called pre-exponential factor, k_B the Boltzmann constant E_A denoting the activation energy. The activation energy is ordered 106, 98.8, and 90 kJ/mol for H30, H50, and H40, respectively.

These values are in good agreement with the data given in refs. 8 and 54 as 115, 98, and 93, respectively. This may reflect unexpecting independence on the generation number i.e., on the molecular weight in such systems of unique architecture. The relatively high values of the apparent activation energies here might be because of the high density of the hydroxyl groups. In other words, the high values of activation energies for such systems could be explained by the high hindrance of the fluctuation of the hydroxyl groups. For the H20 sample, a remarkable deviation from Arrhenius like behavior is observed. The temperature dependence of the
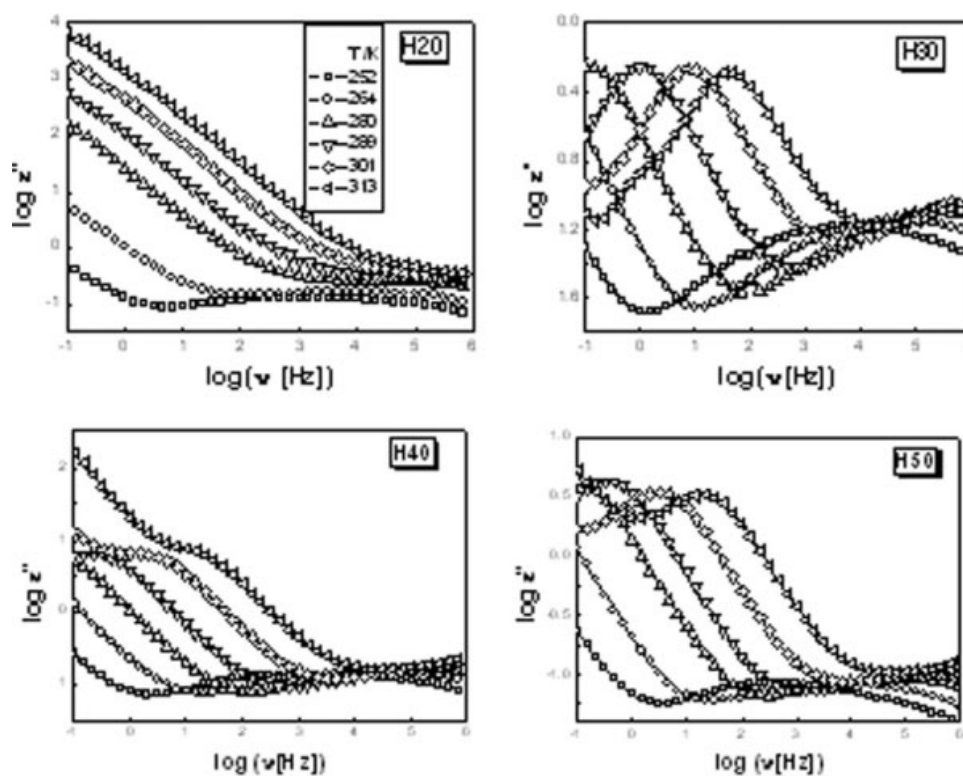
Figure 3 Log–log plots of the imaginary part ε'' of the dielectric function versus frequency ν for the four investigated samples at selected temperatures. [*The symbols in each Figure correspond to the same temperature*].

relaxation rates seems to follow the VFT- model.[57–59] It could be attributed to the higher OH density in this lowest generation which led to stronger intera-molecular interactions rather than the intermolecular ones. This hindered more and more the fluctuation of OH groups which leads in consequence to co-op-erative processes causing the VFT behavior.

β-Process and Conductivity

The β-process is also fitted using the HN-model. It is in cases of H40 and H50 overlaid by a conduc-tivity contribution. Conductivity effects are treated in the usual way by adding a conductivity contri-bution,

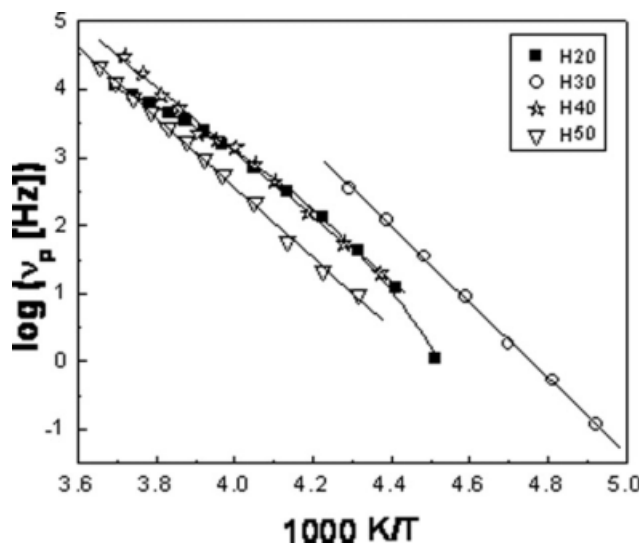$$\frac{\sigma_0}{\varepsilon_0(2\pi\nu)^S}, \qquad (4)$$

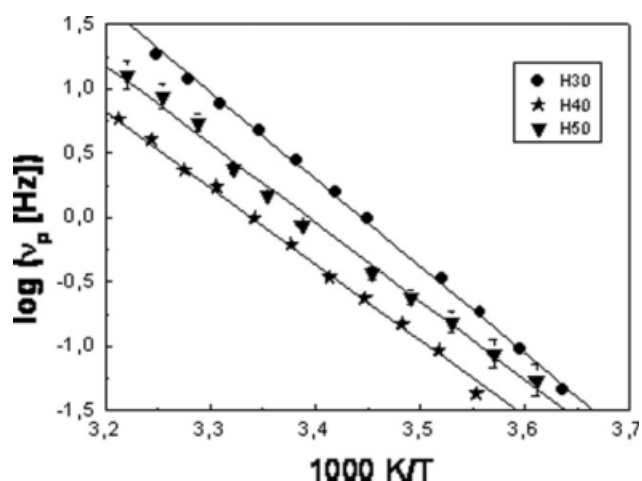**Figure 4** Activation plot of the γ-process for the different investigated generations as labeled.

Figure 5 The activation plot of the β-process for the labeled generations.
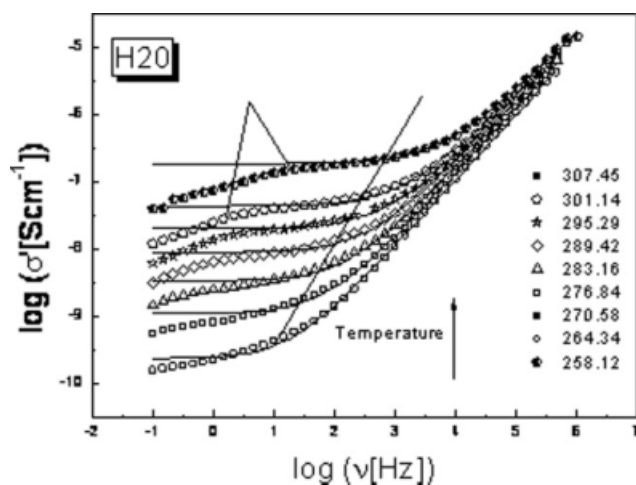
Figure 6 The dependence of the real part of ac-conductivity, σ', on the frequency at significant temperatures in Kelvin of the 2nd generation sample H20.

to the dielectric loss, where σ_0 is related to the dc – conductivity of the sample and ε_0 is the dielectric permittivity of vacuum ($\varepsilon_0 = 8.854 \times 10^{-12}$ As

V^{-1} m^{-1}). The parameter S ($0 < S \leq 1$) describes for $S < 1$ non-Ohmic effects in the conductivity.

The dependence of relaxation rate on the inverse temperature for the β-process is given in Figure 5.

It is clear from the figure that the temperature dependence of relaxation rate for the β-process follows Arrhenius behavior. The β-process of H20 disappears because the strong effect of conductivity and/or electrode polarization as stated previously. The activation energies of the investigated samples are ordered in the same way as for the γ-process H30, H50, and H40 (127, 116, and 114 kJ/mol). This process appears at higher temperatures in comparison with γ-process. It was attributed to the orientation of the ester groups as previously discussed. Although its apparent activation energies is too high to be considered due such localized motions, its values are comparable with that of γ-process. It can be concluded that the molecular dynamics in such polymers with a special architecture are more complicated because of the intra- and inter-molecular interactions and do not follow a generation (molecular weight) dependence.
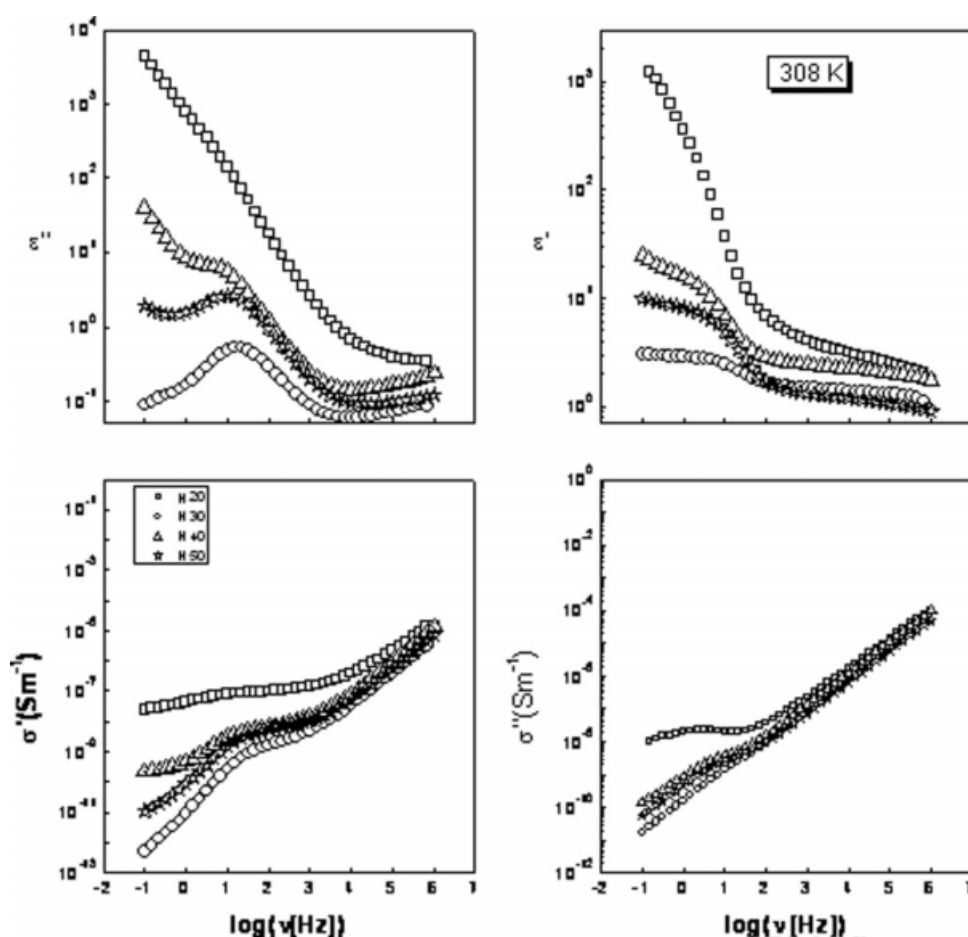

Figure 7 The imaginary and real parts of the complex permittivity and of the complex conductivity (in Ω^{-1} m^{-1}) vs. frequency ν (in Hz) at 308 K for the investigated samples. The symbols correspond to the same generations.

The anomalous large values for the dielectric loss ε'' in the region of low frequency and high temperatures is attributed usually to the ionic conduction and/or electrode polarization. To discriminate between conductivity and electrode polarization it is useful to consider the complex conductivity σ^*. Its relationship to the dielectric relaxation function is given by $\sigma^*(\nu) = i\omega\varepsilon_0\varepsilon^*(\nu)$, with the real part $\sigma'(\nu) = i\omega\varepsilon_0\varepsilon''(\nu)$ and the imaginary part $\sigma''(\nu) = i\omega\varepsilon_0\varepsilon'(\nu)$.

Figure 6 shows the frequency and temperature dependence of the real part of the complex conductivity, σ', for the sample H20. It becomes clear from Figure 6 that σ' has a plateau on the low frequency side which bends off at a certain critical frequency ω_c and results for $\omega \gg \omega_c$ in a power law dependence of the type $\sigma' \sim \omega^s$ ($s \leq 1$). This plateau obtained for σ' can be extrapolated to the dc conductivity for ν tends to zero. The behavior noticed here seems to be the typical of the materials characterized by relatively high conductivity (e.g., ionic glasses,[60,61] ion conducting polymers,[59–61] electron-conducting conjugated polymers[62–64] or conducting carbon black composites[65–68]).

The lines are the fit of Jonscher equation to the data.

The plateau value and the critical frequency ω_c decreases with decreasing temperature [see the longer row in Fig. 6]. This finding may indicate that the dc and ac conductivity are closely related to each other and based on the same mechanism of charge transport. For higher temperatures, there are pronounced signs of electrode polarization- shorter rows. The frequency and temperature dependence of the conductivity shows the well-known universal features of semi conducting disordered materials.

Figure 7 illustrates graphically the frequency dependence of the conductivity and permittivity, (real and imaginary parts), at a fixed temperature 308 K for the four investigated samples. The abrupt increase of ε' with decreasing frequency in bislope like behavior for, H20, at lower frequencies range reflects the superposition of the electrode polarization with the dc conductivity that masked the peak of β-process in $\varepsilon''(\nu)$ spectrum. This is shown in the σ' plot as a plateau for the conductivity followed by a shoulder for the electrode polarization. On the other hand, only pure conductivity could be seen for the other three generations that overlaid the peak of the β-process. The conductivity contribution seems to be very low for the H30 sample.

Jonscher equation[69] eq. (5) is fitted to the data of the frequency dependence of the conductivity for the four investigated polymers

$$\sigma'(\nu) = \sigma_0 + A\nu^S = \sigma_0[1 + (\nu/\nu_c)^S] \qquad (5)$$

Some examples for the fit of eq. (5) to the data were given in Figure 8 for the sample H20 as a represen-
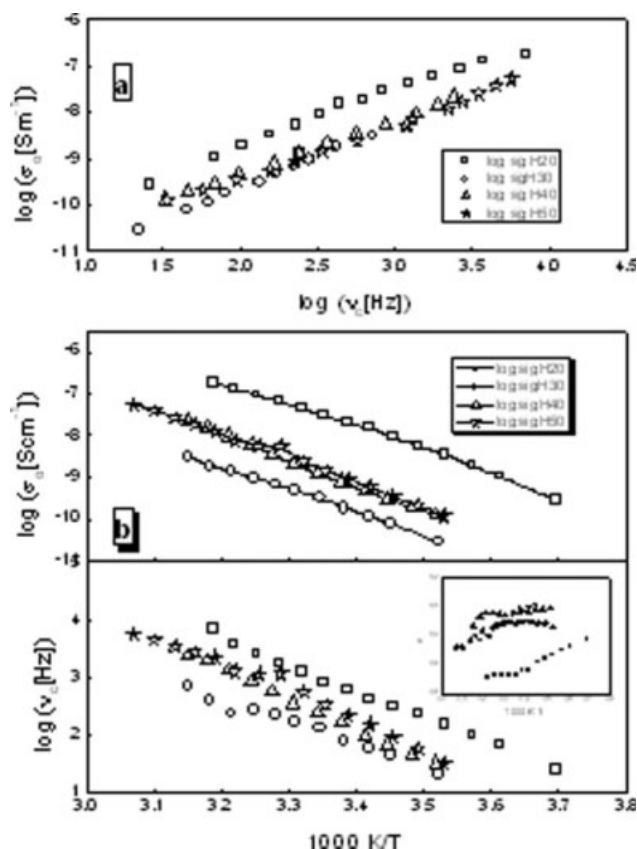

Figure 8 The fit parameters of eq. (5) for the sample H20. (a) DC conductivity vs. characteristic frequency, (b) DC conductivity and the characteristic frequency vs. reciprocal temperature. (Inset) Dispersive index s vs. reciprocal temperature.

tative example. A good description is noticed here over the whole frequency window. The deviation at the lower frequencies is because of the electrode polarisation plays the main role. Figure 8 illustrates graphically the fit parameters. dc conductivity as a function of ν_c shows linear relation for the higher three generations H30, H40, and H50 without any remarkable effect of the molecular weight. This is consequence of the Barton/Nakajima/Namikawa (BNN) relationship.[70] Only the H20 sample shows a deviation from linearity and has higher values of conductivity than the other three samples. This is because of the coincidence between conductivity and electrode polarisation.

CONCLUSION

Molecular relaxation and properties of hyperbranched polyesters of generation varied systematically between 2 and 5 are studied using the Broadband dielectric spectrometer. The generation affect strongly the dielectric properties. The conductivity effect is too high and masks the α-relaxation. The conductivity is systematically analyzed which

obeys the peculiarities found to be characteristic for semiconducting disordered materials. The Barton/Nakajima/Namikawa relationship is found to be valid. Two relaxation processes at lower temperatures than the glass transition one were observed. Both relaxation processes, γ-process at lower temperatures and a β-process at higher ones, have too high apparent activation energies. This is attributed to the complicated structure of such polymers.

References

1. Frechet, J. M. J.; Tomalia, D., Eds. Dendrimers and Other Dendritic Polymers; John Wiley & Sons: 2001.
2. Newkome, G. R.Dendrimers and Dendrons: Concepts, Syntheses, Applications, Wiley – VCH: 2001.
3. Gillies, E. R.; Frechet, J. M. J. DDT 2005, 10, 35.
4. Aulenta, F. Eur Polym J 2003, 39, 1741.
5. Stiriba, S. E.; Holger, F.; Haag, R. Angew Chem Int Ed Engl 2002, 41, 1329.
6. Patri, A. K.; Majoros, J.; Baker, R. Curr Opin Chem Biol 2002, 6, 466.
7. Boas, U.; Heegaard, P. M. H. Chem Soc Rev 2004, 33, 43.
8. Zhu, P. W.; Zheng, S.H; Simon, G. Macromol Chem Phys 2001, 202, 3008.
9. Kim, Y.; Webster, J.WebsterJ. Am Chem Soc 1990, 112, 4592.
10. Voit, B. J Polym Sci 2000, 38, 2505.
11. Beak, J.-B.; Tan, L.-S.U.S. Department Of the Air Force. U.S. Patent 6,707,849, 2005.
12. Stump, J.-F.; Bruchmann, B.; Bedat, J. BASF AG. Wo 101624, 2004.
13. Norihisa, H.; Abe, S.; Kanesato, M. Japanese Patent JP 011901, 2005.
14. Leggio, A. J.; Wood, M. G.; Suhadolnik, J.; McNamara, J. J.; Dog, J. U.S. Patent 005,372, 2005.
15. Clement, F.; Peduto, N.; Touraud, F.; Troc, F.; Lapierre, C. Radio Engineering Plastics S.r.I. French Patent FR 28 56693, 2004.
16. Owens, B. A.; Jakson, N. E.; Collias, D. I. Procter & Gamble Co., U.S. Patent 2,003,212,173, 2003.
17. Baker, A. S.; Walbridge, D. J. Imperial Chemical Industries, Ltd., U.S. Patent 3,669,939, 1972.
18. Hawker, C. J.; Lee, R.; Frechet, J. M. J J Am Chem Soc 1991, 113, 4583.
19. Wooley, K. L.; Hawker, C. J.; Lee, R.; Frechet, J. M. J. Polym J 1994, 26, 187.
20. Kambouris, P.; Hawker, C. J. J Chem Soc Oerkin Trans 1993, 27, 17.
21. Turner, S. R.; Voit, B.; Mourey, T. H. Macromolecules 1993, 26, 4617.
22. Turner, S. R.; Walter, F.; Voit, B.; Mourey, T. H. Macromolecules 1997, 27, 1611.
23. Yamaguchi, N.; Wang, J.-S.; Hewitt, J. M.; Lenhart, W. C.; Mourey, T. J Polym Sci: Part A Polym Chem 2002, 39, 2855.
24. Kricheldorf, H. R.; Stober, O. Macromol Rapid Commun 1994, 15, 87.
25. Malmström, E.; Johansson, M.; Hult, A. Macromolecules 1995, 28, 1698.
26. Hult, A.; Johansson, M.; Malmstroem, E. Adv Polym Sci 1999, 1, 143.
27. Feast, W. J.; Stainton, N. M. J Matwer Chem 1995, 5, 405.
28. Chu, F. K.; Hawker, C. J.; Pomery, P. J.; Hill, D. J. T. J Polym Sci Part A: Polym Chem 1997, 35, 1627.
29. Blencowe, A.; Davidson, L.; Hayes, W. Eur Polym J 2003, 39, 1955.
30. Fuoss, R.; Kirkwood, J. Am Chem Soc 1941, 63, 385.
31. McCrum, N.; Read, B.; Williams, G. Anelastic and Dielectric Effects in Polymeric Solids, Wiley: NY, 1991; reprinted by Dover Publications.
32. Ishida, Y.; Yamafuji, K. Kolloid Z 1961, 177, 97.
33. Ishida, Y.; Matssuo, M.; Yamafuji, K. Kolloid Z 1969, 180, 108.
34. Ishida, Y. J Polym Sci 1969, 27, 1835.
35. Hedvig, P. Dielectric Spectroscopy of Polymers, Adam Hilger: Bristol, 1977.
36. Karasz, F. E. Dielectric Properties of Polymers, Plenum: NY, 1972.
37. Blythe, A. R. Electric Properties of Polymers, Cambridge University Press: Cambridge, 1977.
38. Adachi, K.; Kotaka, T. Prog Polym Sci 1993, 33, 60.
39. Rainde, E.; Saiz, E. Dipole Moments and Birefringence of Polymers, Prentice Hall: Englewood Cliffs, New Jersey, 1992.
40. Williams, G. Adv Polym Sci 1979, 33, 60.
41. Williams, G. In Comprehensive Polymer Science, Allen, G.; Bevington, J. C., Eds. Pergamon Press: 1989; Vol. 1.
42. Williams, G. In Structure and Properties of Polymers, Materials Science & Technology Series, Thomas, E. l., Ed. VCH Publications: 1993; 12: P 471.
43. Runt, J. P.; Fitzgerald, J. J., Eds. Dielectric Spectroscopy of Polymeric Materials, American Chemical Society: Washington, DC, 1997.
44. Schönhals, A.; Kremer, F. Broadband Dielectric Spectroscopy, 1st ed.; Kremer, F.; Schönhals, A., Eds.; 2002, Chapter 42.
45. Turky, G.; Schönhals, A. Polymer 2004, 45, 255.
46. Malmström, E.; Hult, A.; Gedde, U. W.; Liu, F.; Boyd, R. H. Polymer 1997, 38, 4873.
47. Okrasa, L.; Zigon, M.; Zagar, E.; Czech, P.; Boiteux, G. J Non-Cryst Solids 2005, 351, 2753.
48. Czech, P.; Okrasa, L.; Ulanski, J.; Boiteux, G.; Mechin, F.; Cassagnau, P.H. J Appl Polym Sci 2007, 105, 89.
49. Czech, P.; Okrasa, L.; Mechin, F.; Boiteux, G.; Ulanski, J. J Non-Cryst Solids 2005, 351, 2735.
50. Czech, P.; Okrasa, L.; Mechin, F.; Boiteux, G.; Ulanski, J. Polymer 2006, 47, 7207.
51. Serghei, A.; Mikhailova, Y.; Eichhorn, K.-J.; Voit, B.; Kremer, F. J Polym Sci 2006, 44, 3006.
52. Serghei, A.; Mikhailova, Y.; Schick, Huth H.; Eichhorn, K. J.; Voit, B.; Kremer, F. Eur Phys J 2005, 17, 199.
53. Pettersson, B. Properties and Applications of Dendritic Polymers, Perstorp: Swedan, 2001.
54. Malmström, E.; Liu, F.; Boyd, R. H.; Hult, A.; Gedde, U. W. Polym Bull 1994, 32, 679.
55. Havriliak, S.; Negami, S. J Polym Sci 1966, 14, 89.
56. Schlosser, F.; Schönhals, A. Coll Polym Sci 1989, 267, 963.
57. Vogel, H. Phys Zeit 1921, 22, 645.
58. Fulcher, G. J Am Ceram Soc 1923, 8, 339.
59. Tamman, G.; Hesse, G. Anorg Allgem Chem 1926, 156, 245.
60. Angell, C. A. Chem Rev 1990, 90, 523.
61. Rivera, A.; Santamaria, J.; Leon, C. Appl Phys Lett 2001, 78, 610.
62. Epstein, A. J. Handbook of Conducting Polymers, Skotheim, T. A., Ed. Marcel Dekker: NY, 1986; Vol. 2, p 1041.
63. Ngai, K. L.; Randell, R. W. Handbook of Conducting Polymers, Skotheim, T. A., Ed. Chapter 28, p 967.
64. Ruehe, J.; Kroehnke, C.; Ezquerra, M.; Kremer, F.; Wegner, G. Ber Bunsenges Phys Chem 1987, 91, 885.
65. Pelster, R.; Simon, U. Colloid Polym Sci 1999, 277, 2.
66. Connor, M. T.; Roy, S.; Ezquerra, T. A.; Belta-Calleja, F. J. PRB 1998, 57, 2286.
67. Kremer, F.; Ezquerra, M.; Mohammadi, W.; Bauhofer, W.; Vilgis, T. A.; Wegner, G. Solid State Commun 1988, 66, 153.
68. Pelster, R.; Marquardt, P.; Nimtz, G.; Enders, A.; Eifert, H.; Friedrich, K.; Petzholdt, F. Phys Rev 1992, 45, 8929.
69. Jonscher, A. Nature 1977, 267, 673.
70. Dyre, J.; Schroder, T. Rev Mod Phys 2000, 72, 873.